Mol. Cells *33*, 117-126, February 29, 2012
DOI/10.1007/s10059-012-2165-9

Molecules and Cells

Activation of Rice *Yellow Stripe1-Like 16* (*OsYSL16*) Enhances Iron Efficiency

Sichul Lee[1], Nayeon Ryoo[2], Jong-Seong Jeon[2], Mary Lou Guerinot[1], and Gynheung An[3,*]

Graminaceous plants release ferric-chelating phytosiderophores that bind to iron. These ferric-phytosiderophore complexes are transported across the plasma membrane by a protein produced from *Yellow Stripe 1* (*YS1*). Here, we report the characterization of *OsYSL16*, one of the *YS1-like* genes in rice. Real-time analysis revealed that this gene was constitutively expressed irrespective of metal status. Promoter fusions of *OsYSL16* to *β-glucuronidase* (*GUS*) showed that *OsYSL16* was highly expressed in the vascular tissues of the root, leaf, and spikelet, and in leaf mesophyll cells. The OsYSL16-green fluorescence protein (GFP) fusion protein was localized to the plasma membrane. From a pool of rice T-DNA insertional lines, we identified two independent activation-tagging mutants in *OsYSL16*. On an Fe-deficient medium, those mutants retained relatively high chlorophyll concentrations compared with the wild-type (WT) controls, indicating that they are more tolerant to a lack of iron. The Fe concentration in shoots was also higher in the *OsYSL16* activation lines than in the WT. During germination, the rate of Fe-utilization from the seeds was higher in the *OsYSL16* activation lines than in the WT seeds. Our results suggest that the function of OsYSL16 in Fe-homeostasis is to enable distribution of iron within a plant.

INTRODUCTION

Iron is an essential micronutrient with numerous cellular functions for all living organisms. Although Fe is abundant in the earth's crust, it is often unavailable to plants because, at a neutral pH, it tends to form insoluble ferric oxide complexes in aerobic environments (Guerinot and Yi, 1994). Therefore, Fe-homeostasis in the whole organism, as well as in the cells, must be balanced to supply enough Fe for cell metabolism while avoiding excessive, toxic levels.

Plant cells actuate two separate mechanisms for acquiring Fe (Mori, 1999). Reduction-based Strategy I operates mainly in dicotyledonous and non-graminaceous plants, where Fe(III) is reduced to Fe(II) before being transported into the cell by an Fe(II) transporter. Robinson et al. (1999) have cloned *Arabidopsis Fe(III)-chelate reductase* (*FRO2*). After reduction to Fe(II), Fe is transported across the root plasma membrane via Fe(II) transporters (Marschner and Römheld, 1994). AtIRT1 is a major Fe-transporter at the root surface (Henriques et al., 2002; Varotto et al., 2002; Vert et al., 2002). AtIRT2, a close homolog, is located at the intracellular vesicles and, in cooperation with AtIRT1, maintains Fe-homeostasis in root epidermal cells (Vert et al., 2009).

Grasses, such as rice, corn and wheat, use the Chelation-based Strategy II. In response to Fe-deficiency, graminaceous plant cells release phytosiderophores (PSs), which belong to the mugineic acid (MA) family and are derived from the precursor nicotianamine (NA). Molecules bind to Fe(III) and specific plasma membrane transporter proteins import the Fe(III)-PS complexes (Römheld and Marschner, 1986). The molecular mechanism controlling Fe(III)-uptake has been elucidated by cloning the membrane transporter from the maize *yellow stripe 1* (*ys1)* mutant, which shows characteristic interveinal chlorosis (Basso et al., 1994; Curie et al., 2001). Because that mutant is deficient in Fe(III)-PS uptake, it has been suggested that YS1 is the Fe(III)-PS transporter. The YS1 protein is up-regulated by Fe-deficiencies in roots and shoots, and functions as a proton-coupled symporter to transport Fe(III)-PS (Roberts et al., 2004; Schaaf et al., 2004). Yeast and oocyte studies have indicated that YS1 might have other substrates, including Zn, Ni, and Cu (Roberts et al., 2004; Schaaf et al., 2004).

Among the 18 *YS1-like* (*OsYSL*) genes in rice, OsYSL15 transports Fe(III)-deoxymugineic acid (DMA) and Fe(II)-NA (Inoue et al., 2009; Lee et al., 2009). *OsYSL15* expression is strongly induced in the roots and shoots by Fe-deficiency. Under such conditions, *osysl15* mutants exhibit chlorotic phenotypes and have reduced Fe concentrations in their shoots, roots, and seeds, thereby demonstrating roles for OsYSL15 in Fe-uptake and distribution in rice plants (Inoue et al., 2009; Lee et al., 2009). In barley, HvYS1 is a specific transporter for Fe(III)-PS, which is involved in primary Fe-acquisition in the roots (Murata et al., 2006). Other YSL members may play roles in long-distance movement of metals. *OsYSL2*, induced by Fe-deficiency, is localized to the plasma membrane and transports Fe(II)-NA and Mn(II)-NA, but not Fe(III)-DMA (Koike et al., 2004). An RNAi line of *OsYSL2* shows decreased Fe-transloca-

[1]Department of Biological Sciences, Dartmouth College, Hanover, New Hampshire, USA, [2]Graduate School of Biotechnology, Kyung Hee University, Yongin 446-701, Korea, [3]Department of Plant Molecular Systems Biotechnology and Crop Biotech Institute, Kyung Hee University, Yongin 446-701, Korea
*Correspondence: genean@khu.ac.kr

Received August 11, 2011; revised November 16, 2011; accepted November 17, 2011; published online January 3, 2012

Keywords: activation tagging, homeostasis, iron

tion to seeds, lower Fe concentrations in shoots and seeds, and greater accumulation of Fe in the roots (Ishimaru et al., 2010). Plants over-expressing *OsYSL2* also have less Fe-translocation to shoots and seeds, indicating that OsYSL2 is a critical Fe(II)-NA transporter (Ishimaru et al., 2010). OsYSL18 is a transporter of Fe(III)-DMA but not of Fe(II)-NA (Aoyama et al., 2009). Its expression in flowers and the phloem of lamina joints implies that it is involved in translocating Fe in reproductive organs and phloem joints.

In *Arabidopsis*, YSL proteins are not secreted for Fe-uptake. Instead, they are proposed to function in transporting of Fe within a plant through the formation of Fe-NA complexes (Colangelo and Guerinot, 2006; Curie et al., 2001). *AtYSL1* is a shoot-specific gene whose transcript level is increased in response to high-Fe conditions; its expression in young siliques suggests a role for AtYSL1 in Fe-loading to seeds (Le Jean et al., 2005). The *ysl1/ysl3* double mutants exhibit Fe-deficiency symptoms, including interveinal chlorosis and decreased fertility (Waters et al., 2006). Concentrations of Fe, Zn, Cu, and Mn are altered in those double mutants, and seeds accumulate signifycantly less of all those metals except Mn. During leaf senescence, both genes are strongly expressed throughout the leaves, implying that AtYSL1 and AtYSL3 function in moving metal-NA complexes during senescence and seed production. Chu et al. (2010) also have reported that AtYSL1 and AtYSL3 can transport Fe-NA, and that the latter transports Fe-DMA as well. The *AtYSL2*promoter::*GUS* fusion stains xylem-associated cells within the vasculature of expanded leaves. Its broad expression pattern within differentiated roots suggests that AtYSL2 participates in the lateral transport of metals in the veins (Di Donato et al., 2004; Schaaf et al., 2005). Finally, TcYSL3 encodes an NA-Ni/Fe-transporter in the metal hyperaccumulator *Thlaspi caerulescens* (Gendre et al., 2007).

In this study, we showed that the function of OsYSL16 in iron homeostasis is for distribution of Fe within rice plants.

MATERIALS AND METHODS

Plant growth

Wild-type (WT) and transgenic rice seeds were germinated on MS agar plates. The standard medium contained 0.1 μM $CuSO_4$, 100 μM Fe(III)-EDTA, 30 μM $ZnSO_4$, and 10 μM $MnSO_4$ as micronutrients. To test the effect of deficiencies, we germinated seeds and then reared the seedlings on MS media lacking $CuSO_4$ (Cu-deficient), Fe(III)-EDTA (Fe-deficient), $ZnSO_4$ (Zn-deficient), or $MnSO_4$ (Mn-deficient). For RNA analysis, shoot and root samples from 7-day-old seedlings were frozen with liquid nitrogen. Other seedlings were transplanted into soil and grown to maturity in a greenhouse (14-h photoperiod).

RNA isolation and mRNA quantification

Total RNA was isolated from frozen samples with RNAiso Plus (Takara, Japan). For cDNA synthesis, we used 2 μg of total RNA as template and M-MLV reverse transcriptase (Promega, USA) in a 25-μl reaction mixture. RT-PCR was conducted in a 50-μl solution containing a 1-μl aliquot of the cDNA reaction, 0.2 μM of gene-specific primers, 10 mM dNTPs, and 1 unit of rTaq DNA polymerase (Takara). The PCR products were separated by electrophoresis on a 1.2% agarose gel. Gene-specific primers for the *OsYSL* gene family are listed in Supplementary Table I. Real-time PCR was performed with a Rotor-Gene 6000 real-time rotary analyzer (Corbett Life Science, Australia) and a SYBR premix Ex Taq kit (Takara). Levels of *actin1* mRNA were used to normalize the expression ratio for each gene. Changes in expression were calculated *via* the cycle threshold ($\Delta\Delta_{Ct}$) method.

Genotyping *OsYSL16* mutant plants

One insertional mutant line (1A13505) and two activation-tagging lines (1B04137 and 2D00022) for *OsYSL16* were isolated from our T-DNA flanking sequence tag database (An et al., 2003; Jeong et al., 2006). For genotyping of the knockout mutant (*osysl16-1*), we used two gene-specific primers (F1, 5′-CTGGGGCTGAACAAGAAGAC-3′ and R1, 5′-GATGCCGAA ATACCTGAGGA-3′) and a T-DNA-specific primer (LB, 5′-AC GTCCGCAATGTGTTATTAA-3′). For Line 1B04137 (*OsYSL16-D1*), two gene-specific primers (F2, 5′-ACATGAGGTTTGCA TTTGCGTAC-3′ and R2, 5′-GAGACGACGATCAGACGAACG-3′) and a T-DNA-specific primer (LB, 5′-ACGTCCGCAATGT GTTATTAA-3′) were used. Line 2D00022 (*OsYSL16-D2*) required two gene-specific primers (F3, 5′-TGGGCTTCTAAAG TTTGGATT-3′ and R3, 5′-GCCAAAGTCCTTCACTTTCTC-3′) and a T-DNA-specific primer (RB, 5′-CAAGTTAGTCATGTAA TTAGCCAC-3′). Levels of *OsYSL16* transcript were determined by RT-PCR, using cDNA prepared from the leaves of 10-day-old seedlings.

Generation of *OsYSL16* promoter::*GUS* fusion transgenic plants, and *GUS* assays

Genomic sequences (-1,700 bp to -1 bp from the translation initiation site) containing the promoter region of *OsYSL16* were amplified by PCR, using two primers (pf, 5′-AAAAGCTTAATT AAGATCGCGTAGATTGAA-3′ and pr, 5′-AAGGATCCCTGCC GGCCGCACCCGACGAGGC-3′). This fragment was connected to the promoterless *GUS* gene (derived from pBI 101.2) and ligated into pCAMBIA1302, resulting in pGA2865. The new plasmid was transferred to *Agrobacterium tumefaciens* strain LBA4404 by the freeze-thaw method (An et al., 1988). Transgenic plants carrying the above construct were generated via *Agrobacterium*-mediated co-cultivation (Lee et al., 1999). Histochemical *GUS*-staining of the transgenic plants was performed according to the procedure described by Lee et al. (2009). Afterward, 10-μm sections were prepared and observed with a microscope (Nikon, Japan) under bright and dark-field illumination.

Sub-cellular localization of the OsYSL16-GFP fusion protein

The cDNA fragment spanning the entire ORF of *OsYSL16* was amplified with primers Y16-pgf (5′-AAAGATCTCCGCCACGCG CTGGGCGGCGGT-3′; added *Bgl*II site is underlined) and Y16-pgr (5′-AAACTAGTGTTTCCCGGTATGAACTTCAT-3′; *Spe*I site underlined). After being digested with both *Bgl*II and *Spe*I, it was inserted into the *Bgl*II /*Spe*I-linearized pCAMBIA1302 vector. The resulting construct, pGA2886, containing the fusion of OsYSL16-GFP under the CaMV*35S* promoter, was confirmed by sequencing. The vector was then transferred to *A. tumefaciens* strain LBA4404 and introduced into rice as described above. Transgenic progeny plants were grown on sterile solid MS and collected at 5 days after germination. Their roots were examined by laser-scanning confocal microscopy (LSM 510 META, Carl Zeiss, Germany). GFP signals were detected by exciting at 488 nm from an argon laser and collecting emission at 522 nm.

Generation of *OsYSL16*-antisense transgenic plants

For our *OsYSL16* antisense construction, its gene-specific sequence located at the 3′ end was amplified by primer pair anF (5′-AAGGTACCACAGCGACTGCTGTTCTCATAA-3′) and anR (5′-AAGAGCTCCGCCTTGTAGAAGAGGAAGAAG-3′). The

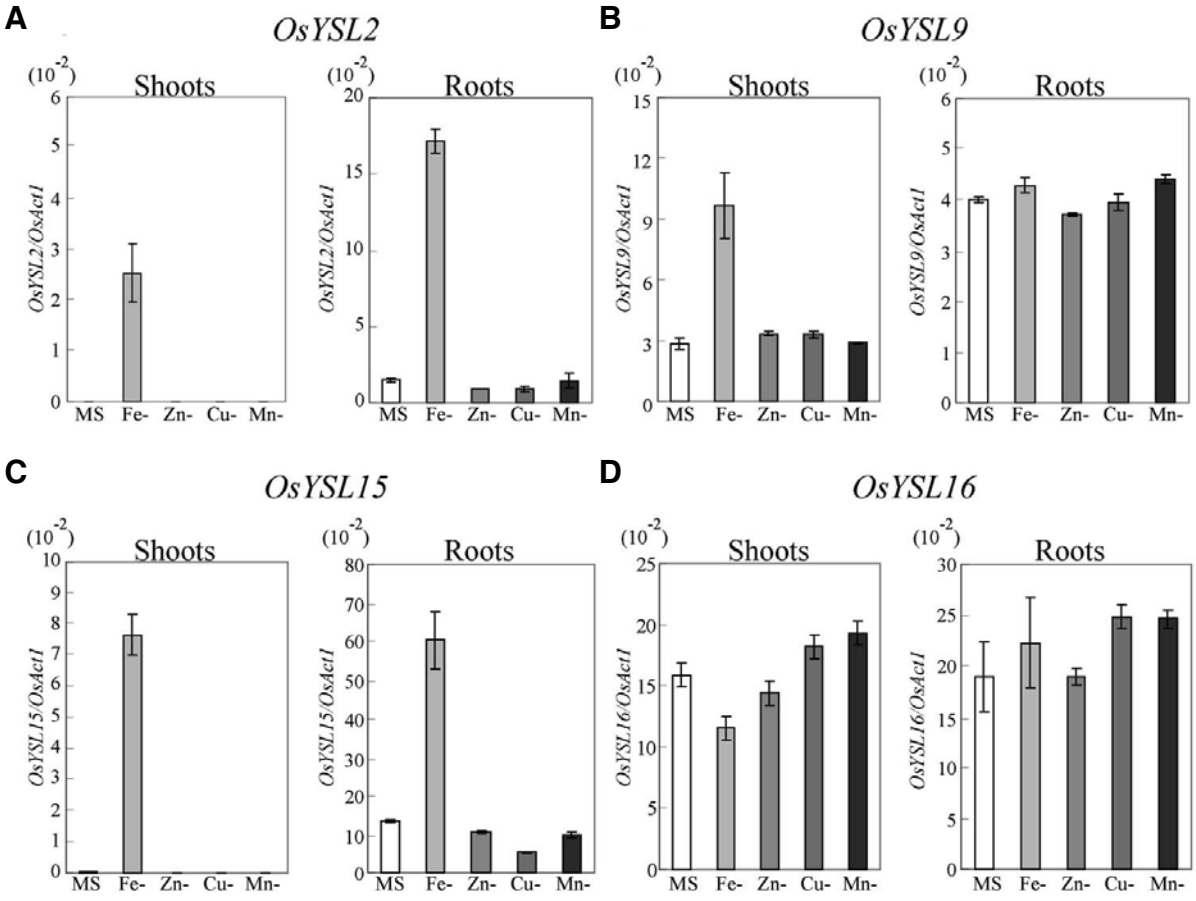

Fig. 1. Expression analyses of *OsYSL* genes under micronutrient-deficient conditions. Seedlings were grown for 7 d on MS medium containing standard amounts of micronutrients [0.1 μM $CuSO_4$, 100 μM Fe(III)-EDTA, 30 μM $ZnSO_4$, and 10 μM $MnSO_4$]. For deficiency tests, seeds were germinated and seedlings grown for 7 d in MS medium lacking Fe(III)-EDTA (Fe-deficient), $ZnSO_4$ (Zn-deficient), $CuSO_4$ (Cu-deficient), or $MnSO_4$ (Mn-deficient). Transcript levels are presented as ratios between mRNA levels of *OsYSL2* (A), *OsYSL9* (B), *OsYSL15* (C), or *OsYSL16* (D) and those of rice *actin1*. Vertical bars indicate standard deviation. Each value is average of 3 independent experiments.

PCR product was cut with *Kpn*I and *sac*I, then ligated into the maize *Ubiquitin1* (*Ubi1*) promoter of pGA1611, thereby generating pGA2876 (Lee et al., 1999). For RNA gel blot analysis, total RNAs were isolated from seedling leaves with an RNA isolation kit (Tri Reagent, USA). The isolated total RNAs were fractionated on a 1.3% agarose gel, blotted onto a nylon membrane, and hybridized with a ^{32}P-labeled probe (Kang et al., 1998).

Measurements of plant growth and metal concentrations

Seeds of WT and mutant plants were germinated and seedlings grown on a solid medium containing MS salts with or without 100 μM Fe(III)-EDTA. For determining chlorophyll concentrations, the leaves were harvested and chlorophyll was extracted with 1 ml of 80% acetone from 0.1-g samples. After homogenization, the samples were incubated for 15 min and spun at 15,000 *g* for 10 min. An aliquot of supernatant fraction was then taken to measure the A_{663} and A_{643} with a spectrophotometer. Chlorophyll concentrations, including chlorophyll a and b, were obtained according to the method of Arnon (1949). For measuring levels of Fe, Zn, Cu, and Mn, the seeds, shoots, and roots were dried separately for 2 days at 70°C before being weighed. Samples were then digested in 1 ml of 11 N HNO_3 for 3 days. After dilution, their metal concentrations were determined by atomic absorption spectroscopy (AAS; SpectraAA-800, USA).

RESULTS

Expression analysis of four *OsYSL* genes under different metal statuses

A database search for rice genome sequences identified a family of 18 genes that are similar to maize *YS1* (Koike et al., 2004). Among them, *OsYSL2*, *OsYSL9*, *OsYSL15* and *OsYSL16* are grouped with *YS1.* Previously, we showed that, except for *OsYSL16*, transcripts of those genes are increased when Fe is limited (Lee et al., 2009). In this study, we studied expression patterns under various metal-deficient conditions.

Seedlings were grown for 7 days on an MS medium containing either standard amounts of micronutrients or else lacking Fe, Zn, Cu, or Mn. Afterward, gene expression was comprehensively examined by quantitative real-time PCR (Fig. 1). In shoots, transcript levels for *OsYSL2* and *OsYSL15* were very low when plants were grown under mineral-rich conditions, but were strongly induced by Fe-deficiency. Similar results were achieved when evaluating the roots. These observations suggest

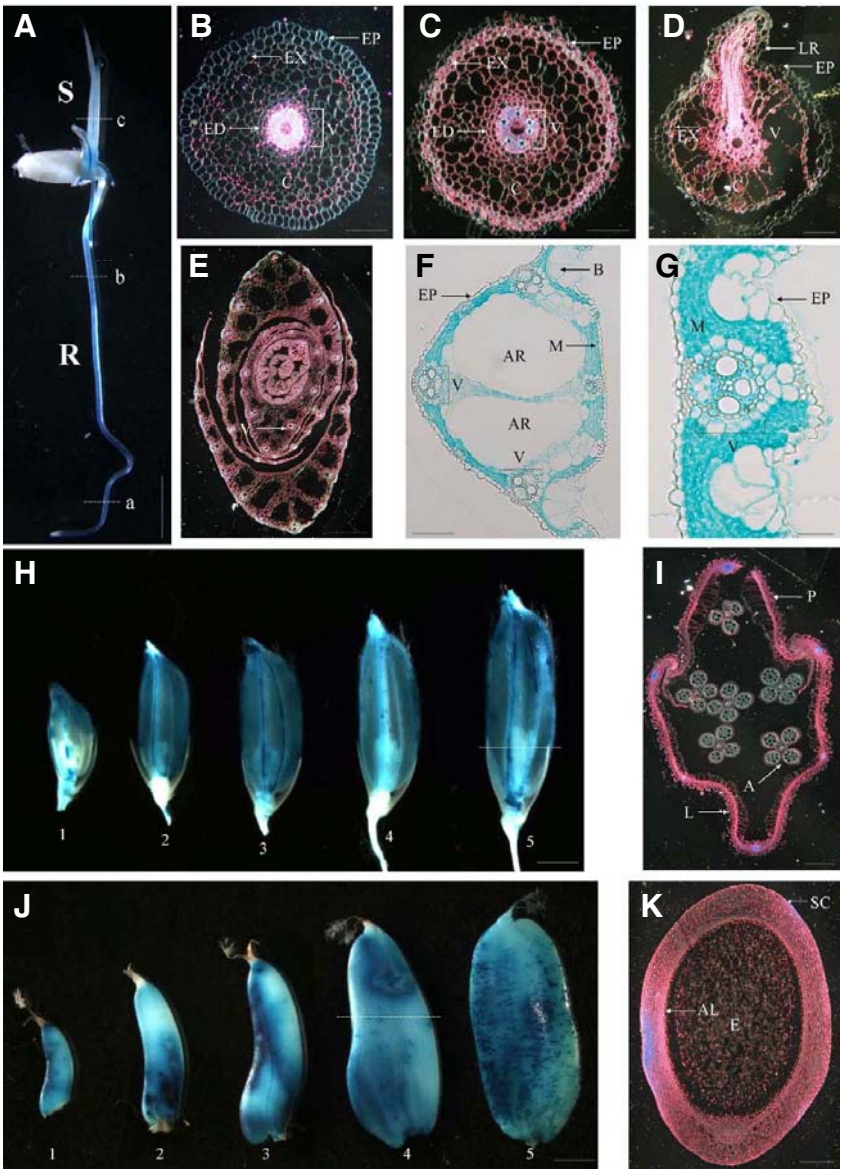

Fig. 2. *OsYSL16* promoter-driven *GUS* expression pattern. (A) Five-day-old seedling grown on MS medium. S, shoots; R, roots. (B-G), Cross sections of (B) 5-day-old seedling root at dividing zone (a in Fig. 2A), (C) differentiation zone (b in Fig. 2A), (D) lateral root from 10-day-old seedling, (E) shoot (c in Fig. 2A), (F) midrib region of leaf, and (G) leaf blade. (H) Temporal and spatial expression patterns of *OsYSL16*::*GUS* fusion construct in spikelets at various stages, as defined by extent of anther development. Samples; 1, tetrad; 2, early young microspore; 3, late young microspore; 4, vacuolated pollen; and 5, late pollen mitosis. (I) Cross section of Sample 5 in (H) at indicated position. (J) Analyses of *GUS* activity in developing seeds. Samples; 1, 3 DAP (days after pol-lination); 2, 5 DAP; 3, 7 DAP; 4, 10 DAP; 5, 20 DAP. (K) Cross section of Sample 4 in (J) at indicated position. (B), (E), (I), and (K) are dark-field images where *GUS* activities are visualized as red signals. In other panels, *GUS*-staining is shown in blue. A, anther; AL, aleurone layer; AR, aerenchyma; B, bulliform cell; C, cortex; E, endosperm; ED, endodermis; EP, epidermis; EX, exodermis; L, lemma; LR, lateral root; M mesophyll; P, palea; R, roots; S; shoots; SC, seed coat; V, vascular bundle. Bars = 1 cm in A; 50 μm in B-G; 1 mm in H, J; 100 μm in I, K.

that both genes are needed when Fe is limiting. Likewise, *OsYSL9* was induced by Fe-deficiency in the shoots but not the roots. By contrast, *OsYSL16* was constitutively expressed in both roots and shoots at levels similar to those of the other three genes, but altering the Fe status had no remarkable effect on the expression of that gene. These observations coincide with those we previously reported (Lee et al., 2009). As for the other micronutrients (i.e., Cu, Zn, and Mn), their deficiencies elicited no such gene response under our experimental conditions (Fig. 1).

We selected *OsYSL16* for further study because it had not yet been characterized in detail.

Expression analysis of the *OsYSL16* promoter in transgenic rice

To examine various spatial and temporal expression patterns, we fused the 1.7-kb fragment carrying the *OsYSL16* promoter to *GUS* and generated transgenic plants that expressed this construct. Histochemical GUS-staining of 5-day-old seedlings showed that, consistent with our quantitative real-time PCR analysis, GUS activity was detected in seedling shoots and roots under normal growing conditions (Fig. 2A). For example, in the cross sections of seminal roots, strong activity was observed in the vascular cylinder (Fig. 2B). Within the differentiation zone, *GUS* expression was expanded to all regions except the epidermis (Fig. 2C). In lateral roots, activity was abundant in vascular bundle tissues (Fig. 2D) whereas the seedling shoots showed higher activity in younger leaves (Fig. 2E), where it was detected mainly in the vascular bundles and mesophyll cells but absent in the epidermis (Figs. 2F and 2G). In developing spikelets, GUS activity was constitutively detected at all developmental stages (Fig. 2H). Cross sections of flowers showed that activity was weak in the anther walls but detectable in the palea/lemma, particularly in the vascular bundle tissues (Fig. 2I). In developing seeds, all tissues had activity, including the embryo, seed coat, and endosperm (Figs. 2J and 2K).

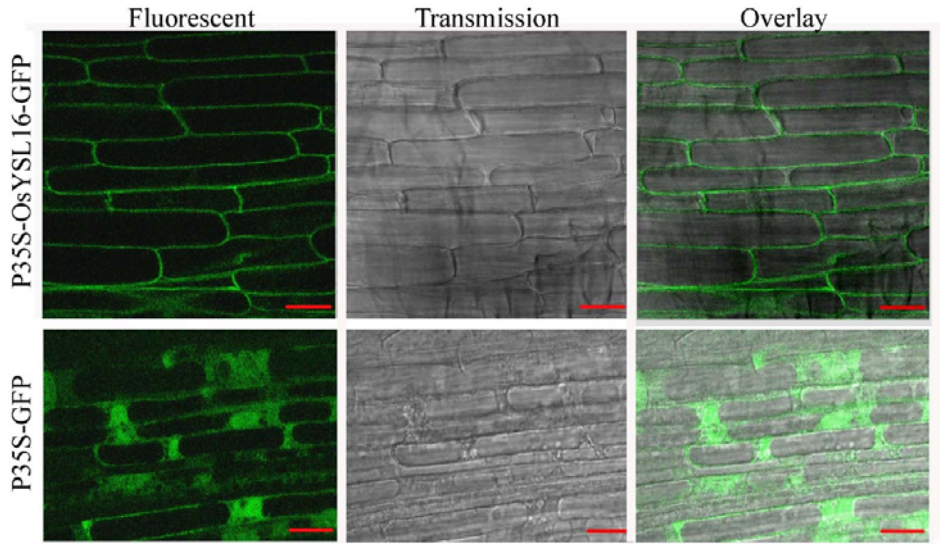

Fig. 3. Sub-cellular localization of OsYSL16-GFP fusion protein. Full-length *OsYSL16* cDNA was fused to *GFP* in same reading flame and resulting construct was transferred to *Agrobacterium tumefaciens* for rice transformation. Representative fluorescence microscopic images of roots expressing OsYSL16-GFP fusion protein are shown. GFP fluorescence was detected at plasma membrane. Roots expressing *GFP* under con-trol of CaMV*35S* promoter (P*35S*-GFP) were used as controls. GFP fluorescence in control was detected in cytosol and nuclei. Fluorescence (left) and bright-field (mi-ddle) images are overlaid at right.

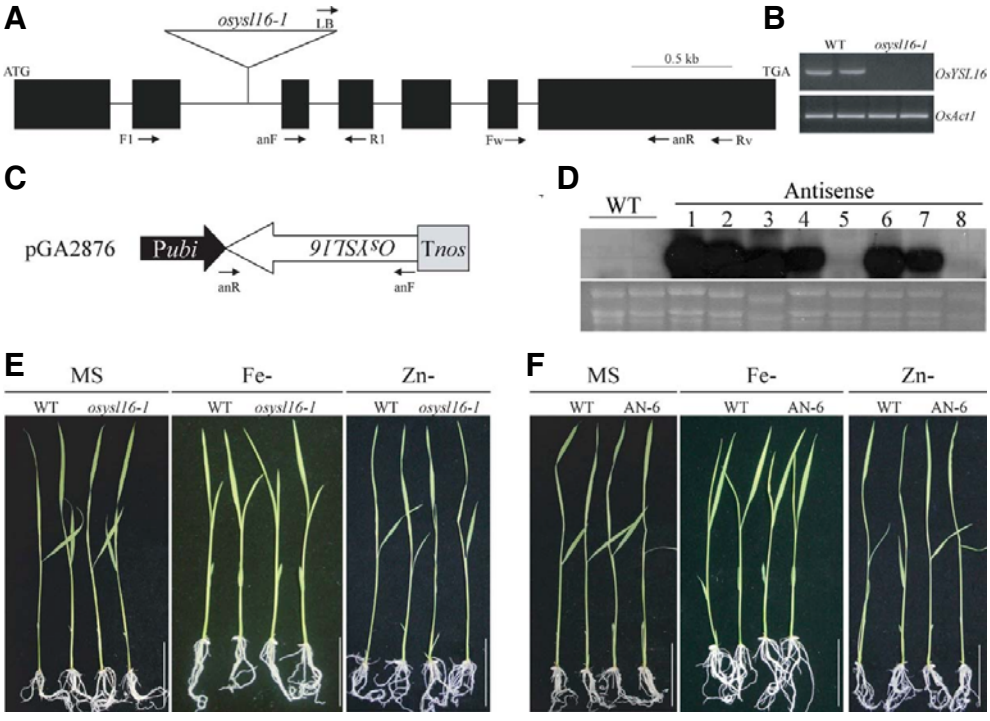

Fig. 4. Isolation of loss-of-function mutant in *OsYSL16* and generation of antisense transgenic plants. (A) Schematic diagram of T-DNA insertion site in *osysl16-1*. Dark boxes show 7 exons; connecting black lines are 6 introns. T-DNA was inserted into 2nd intron. F1 and R1 are gene-specific primers, and LB is T-DNA-specific primer for genotyping. Fw and Rv are gene-specific primers for RT-PCR analysis. (B) RT-PCR analyses of *OsYSL16* expression using *OsYSL16*-specific primers (Fw and Rv). Total RNA was prepared from *osysl16-1* and WT seedlings. Rice *Actin1* (*OsAct1*) mRNA was amplified to show equal loading of RNA in each sample. (C) Schematic diagram of pGA2876 expressing *OsYSL16*-antisense transcripts under control of maize *Ubiquitin* promoter (P*ubi*). anF and anR are gene-specific primers for generation of antisense construct. (D) RNA gel blot analysis of *OsYSL16*-antisense transgenic plants. A gene-specific region amplified by primers anF and anR was used as probe. Two WT and eight independent transgenic plants were examined. The rRNA levels are shown as controls (bottom). (E) and (F) Phenotypes of WT plants, *osysl16-1*, and *OsYSL16*-antisense transgenics (AN-1) germinated and grown on control MS (MS), Fe-deficient (Fe-), or Zn-deficient (Zn-) media for 10 days. Bars = 5 cm.

OsYSL16 is localized in the plasma membrane

Because micronutrients are transported not only across the plasma membrane but also inside cellular compartments, we analyzed the cellular localization of OsYSL16. The PSORT program (http://psort.nibb.ac.jp) predicted, with high probability, that OsYSL16 was located in the plasma membrane. To confirm this prediction, we constructed a chimeric molecule encoding a fusion between OsYSL16 and GFP. In plants stably transformed with the construct, a GFP signal was found in the plasma membrane (Fig. 3). In contrast, fluorescence of GFP alone was observed in the cytosol and nuclei. Thus, we could conclude that this protein was responsible for metal transport in the plasma membrane.

Isolation of a *OsYSL16* knockout mutant and generation of *OsYSL16* antisense lines

Mutants are valuable tools for revealing the roles of a particular gene in physiological and developmental processes. From our rice flanking sequence-tag database (An et al., 2003; Jeong et al., 2006), we identified a mutant line, *osysl16-1* (1A13505), in which T-DNA is inserted in the 2nd intron of *OsYSL16* (Fig. 4A). T2 progeny were obtained and homozygous knockout plants were selected by PCR, using gene-specific primers and T-DNA primers. We demonstrated that *OsYSL16* transcription was disrupted in *osysl16-1* (Fig. 4B).

To evaluate the functional roles of OsYSL16 in Fe and Zn transport, we germinated seeds from WT and *osysl16-1* plants and grew their seedlings on either a standard MS medium or media lacking Fe or Zn. Regardless of growing conditions, phenotypes were indistinguishable between mutants and WT plants, and heights and chlorophyll concentrations were not altered (Fig. 4E; Supplementary Figs. S1A and S1B). To assess whether the disruption of *OsYSL16* affects distribution of Fe and Zn, we measured their levels in shoots and roots at various developmental stages. Concentrations of iron did not differ significantly between genotypes when the Fe supply was either sufficient or deficient (Supplementary Fig. S1C). For zinc as well, plants under either sufficient or deficient conditions showed no changes in concentrations regardless of genotype (Supplementary Fig. S1D).

Because *OsYSL16* promoter activity was detected during flower and seed development (Figs. 2H and 2J), we postulated that disruption of that gene might affect Fe and Zn accumulations in the grains. However, concentrations of these minerals were similar between WT and *osysl16-1* seeds (Supplementary Figs. S1E and S1F).

To confirm our results with the *OsYSL16* loss-of-function mutant, we generated eight independent transgenic plants expressing *OsYSL16* in an antisense orientation under the control of the maize *Ubi1* promoter (Fig. 4C). Their antisense transcript levels were determined by Northern blot analysis using RNA samples prepared from transgenic leaves (Fig. 4D). From the six lines that strongly expressed the antisense transcript, we selected Lines #1 (AN-1) and #6 (AN-6) for further analysis. No remarkable differences in plant heights or chlorophyll concentrations were found between the WT and antisense transgenic plants grown in the absence or presence of Fe or Zn (Fig. 4F; Supplementary Figs. S1A and S1B). Moreover, antisense suppression of *OsYSL16* did not affect the Fe and Zn concentrations in seeds of AN-1 and AN-6 (Supplementary Figs. S1E and S1F).

We also analyzed Cu and Mn distributions in WT and *osysl16* mutant plants. Under deficiencies of either, no phenotypic alterations were apparent (data not shown). Levels of Cu and Mn were also unchanged in the shoots, roots, and mature seeds (data not shown). Therefore, all of these results indicate that another gene(s) must compensate for the deficiency of *OsYSL16* in response to some metals.

Isolation of activation-tagging mutants of *OsYSL16*

Because our loss-of-function approaches did not provide any useful information toward understanding the roles of *OsYSL16*, we isolated activation-tagging mutants to study gain-of-function. In Line 1B04137 (*OsYSL16-D1*), the *35S* 4× enhancer elements were inserted approximately 0.9 kb upstream from the *OsYSL16* coding region (Fig. 5A). For Line 2D00022 (*OsYSL16-D2*), those elements were about 6.5 kb downstream of *OsYSL16* (Fig. 5A). In these lines, *OsYSL16* was a reasonable candidate for the activation-tagging gene. T2 progeny were obtained and homozygous plants were selected by PCR using gene-specific primers and a T-DNA primer (Fig. 5A). Subsequent quantitative real-time PCR analysis revealed that, compared with the control, transcript levels of *OsYSL16-D1* and *OsYSL16-D2* were increased by 7.7- and 2.9-fold in the leaves, and by 7.0- and 3.2-fold in the roots, respectively (Fig. 5B).

Characterization of *OsYSL16* activation-tagging mutants

Homozygous activation-tagging plants of *OsYSL16-D1* and *OsYSL16-D2*, and their co-segregating WT progeny, were grown on either a standard MS medium or one lacking Fe or Zn. Heights and chlorophyll concentrations did not differ between the mutants and the WT for plants on the standard medium or those grown under a Zn-deficiency (Figs. 5C and 5D; Supplementary Figs. S2A and S2C). Likewise, when Cu or Mn was lacking, the WT plants were indistinguishable from the activation-tagging mutants (data not shown).

However, when Fe was deficient, the homozygous activation plants were eventually greener than the control (Figs. 5C and 5D; Supplementary Figs. S2A and S2C). For example, at 4 DAG, no differences were found between WT and activation-tagging plants when Fe was lacking in the medium. By 7 DAG, leaf chlorosis had appeared and chlorophyll concentrations were reduced in plants grown under Fe-limiting conditions. However, the chlorophyll concentration was about 10% higher in the mutants. At 10 DAG, the activation-tagging plants had accumulated at least 20% more chlorophyll compared with the WT, indicating that the *OsYSL16-D* plants were more tolerant of an Fe-deficiency.

Activation of *OsYSL16* affects Fe distribution

We evaluated Fe and Zn concentrations for 10 days in plants grown on either standard or deficient media. For the standard MS medium, Fe levels in shoots and roots were similarly increased for both mutant and WT plants (Fig. 6A). In Fe-deficient media, Fe concentrations did not differ between genotypes at 4 DAG (Fig. 6B). However, at 7 and 10 DAG, the *OsYSL16-D1* plants contained more Fe in the shoots but less in the roots compared with the segregating WT control (Fig. 6C). These results suggested that activation of *OsYSL16* causes enhanced translocation of Fe from roots to shoots.

Over time, Zn concentrations remain relatively constant in shoots but decreased in roots (Supplementary Fig. S3A). In the Zn-deficient medium, *OsYSL-D1* plants contained the same amount of Zn as from the WT (Supplementary Fig. S3B). Levels of Cu and Mn were also unchanged in the shoots and roots of either type (data not shown). Therefore, OsYSL16 does not appear to play a role in transporting Zn, Cu, or Mn in rice plants.

Because *OsYSL16* is actively expressed during seed development (Fig. 2J), we measured mineral levels in mature grains to elucidate how enhanced expression might influence micronutrient storage. Here, Fe, Zn, Cu, and Mn concentrations were similar among the WT and two activation-tagging plants (Figs. 6C and 6D). Moreover, individual seed weights were not significantly different between transgenics and the WT (data not shown). This indicated that the increased Fe concentration in *OsYSL16-D1* shoots was not due to a higher amount of stored Fe in mature seeds. Therefore, it was more likely that Fe-translocation to the shoots was more efficient in the mutants. To verify this hypothesis, we measured Fe concentrations in seeds from plants grown on an Fe-deficient medium. As expected, the level of Fe was more rapidly decreased in *OsYSL16-D1* seeds compared with the segregating WT controls (Fig. 6E). However, Zn levels did not differ between *OsYSL16-D1* and the WT (Supplementary Fig. S3C). These results supported our suppo-

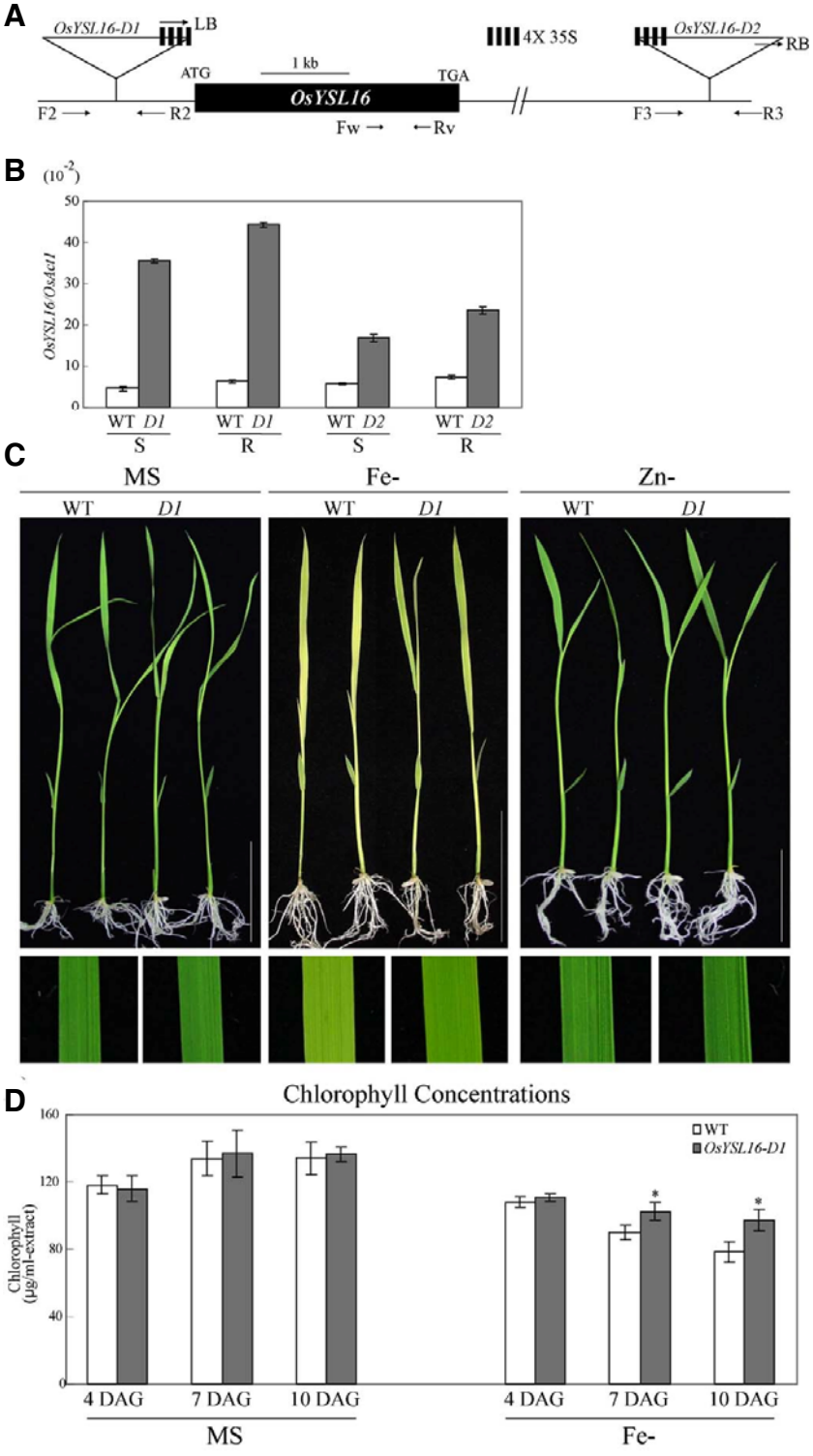

Fig. 5. Phenotypes of *OsYSL16* activation-tagging mutants. (A) Schematic representation of T-DNA insertion sites in *OsYSL16-D1* and *OsYSL16-D2* plants. Primers (F2, F3, R2, R3, LB, and RB) used for genotyping are shown by horizontal arrows. 4 × *35S* denotes 4 copies of *35S* enhancer element. (B) Quantitative real-time PCR analyses of WT and mutant seedlings using gene-specific primers (Fw and Rv) and RNA samples from shoots (S) and roots (R). Transcript levels are presented as ratios between mRNA levels of *OsYSL16* and those of rice *actin1*. *D1* and *D2* indicate *OsYSL16-D1* and *OsYSL-D2* plants; WT means segregating WT plants. Vertical bars indicate standard deviation. Each value is average of 3 independent experiments. (C) Phenotypes of *OsYSL16-D1* at seedling stage under Fe- and Zn-deficiencies. Lower panels are enlargements of second leaves. Pictures were taken 10 d after germination. Bar = 5 cm. (D) Total chlorophyll concentrations from WT plants and *OsYSL16-D1* mutants grown under Fe-sufficient (MS) or -deficient (Fe-) conditions for 4 to 10 DAG. Data are from 2 independent experiments. In each, 4 plants were used for measuring chlorophyll. Error bars represent SE. Significant differences from WT were determined by Student's *t*-test. *, $P < 0.05$.

sition that *OsYSL16* functions to mobilize Fe preferentially to the shoots.

DISCUSSION

In this study of rice, we demonstrated that enhanced tolerance to a low-Fe environment can be achieved through overexpression of *OsYSL16*. This gene is one of four that are closely related to maize *YS*, which encodes an Fe(III)-PS transporter (Koike et al., 2004). Here, expression of *OsYSL2*, *OsYSL9*, and *OsYSL15* was induced by Fe-deficiency whereas transcript levels of *OsYSL16* were relatively constant under either suffi-

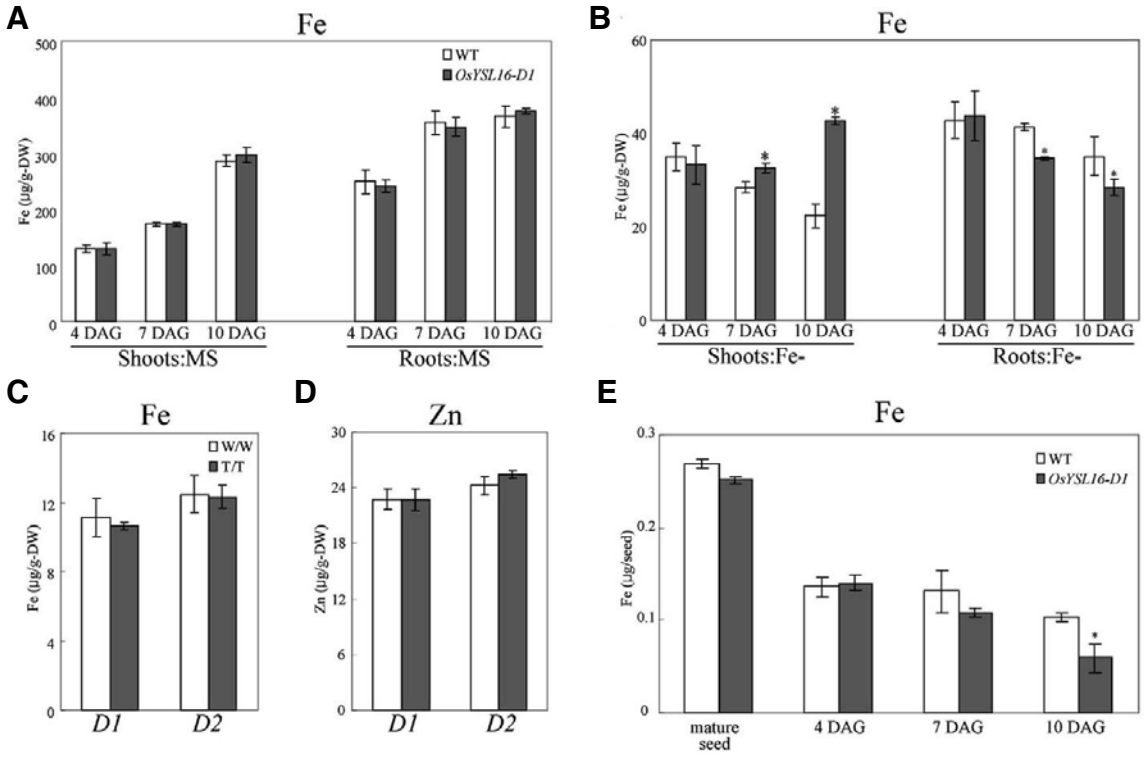

Fig. 6. Phenotypic analyses of WT and *OsYSL16-D1* plants. (A, B), Fe concentrations in shoots and roots of WT and mutants grown for 10 days in Fe-sufficient (MS) or Fe-deficient (Fe-) medium. Fe (C) and Zn (D) concentrations in mature seeds. Fe (E) concentrations from mature seeds and from seeds of 4-10 DAG seedlings grown under Fe-deficient conditions. Error bars represent SE. Significant differences from WT were determined by Student's *t*-test. *, $P < 0.05$.

cient or deficient conditions (Fig. 1). Both *OsYSL2* and *OsYSL15* are very close together on Chromosome 4 while *OsYSL9* and *OsYSL16* are closely located on Chromosome 2. The protein sequences of OsYSL2 and OsYSL15 are 72% identical to each other; those of OsYSL9 and OsYSL16 are 74% identical. These findings indicate that gene duplication occurred during recent genome evolution and that functioning is redundant.

In fact, a knockout mutation and antisense suppression of *OsYSL16* did not cause any alteration in Fe distribution and utilization (Fig. 4; Supplementary Fig. S1). This was likely due to functional redundancy. OsYSL16 and OsYSL9 are highly homologous, closely located, and show a similar induction pattern in roots by external metal supply. These suggest that OsYLS9 could complenent the loss of OsYSL16. To test this hypothesis, generation of the double knock-out of these two genes will be needed. Insertion mutagenesis usually generates recessive loss-of-function mutations, making them unsuitable for functional analysis of redundant genes. Because many rice genes are members of a multigene family (Goff et al., 2002; Yu et al., 2002), researchers must utilize alternative tools for their investigation. Activation-tagging is one method for evaluating the function of redundant genes because the effect is dominant. From a pool of rice T-DNA insertion lines, we obtained two independent activation-tagging lines with enhanced expression of *OsYSL16*. To analyze the phenotypes of these mutants, we tested their tolerance to Fe-deficiency by growing the plants on a medium lacking iron. Visual differences between *OsYSL16-D* and the WT were also reflected in their chlorophyll concentrations and, therefore, the former were deemed more tolerant of that deficiency. Under those conditions, the Fe concentration was higher in the shoots of *OsYSL16*-activated mutants than in the WT plants, and the mutants also had a more rapid rate of Fe-mobilization from seeds to shoots. Ferritin is the major iron stroage protein in all living orgisms (Harrison and Arosio, 1996). In the shoots of *OsYSL16*-activiated mutants, transcript levels of rice *ferriitn* genes were higher than those of WT (data not shown), corresponding with the increased level of Fe in the transgenic shoots. However, *OsYSL16-D* plants did not show any phenotypic differences under deficiencies of Zn, Cu, or Mn (Figs. 5 and 6; Supplementary Figs. S2 and S3). Therefore, these results suggest that OsYSL16 functions to distribute Fe preferentially within a plant.

Ectopic expression of *OsYSL16* also recovered the Fe-deficiency (data not shown). However, the extent of that rescue was weaker compared with expression in the activation-tagging lines. Such ectopic expression alters the original pattern when a foreign promoter is used. In contrast, activation-tagging generally upholds the characteristics of the target genes (Jeong et al., 2006). Therefore, it appears that maintaining a proper expression pattern is a more efficient way to achieve the enhanced effects conferred by a gene.

Previoulsy, we showed that overexpression of two rice Fe transpoters, *OsIRT1* and *OsYSL15*, resulted in shorter heights and fewer tiller than WT when grown in the paddy field (Lee and An, 2009; Lee et al., 2009). However, transgenics from *OsYSL16*-activated mutants and overexpressors did not show any alteration in plant architecture.

Although *OsYSL16* is expressed in many cell types, it is more preferentially expressed in the vascular tissues of roots and leaves. This pattern is similar to that of *AtYSL2,* which is

expressed most strongly in the vascular tissues of leaves and primary roots (Di Donato et al., 2004; Schaff et al., 2005). *AtYSL1* is expressed in the xylem parenchyma of leaves, where it is up-regulated in response to excess Fe, as well as in pollen and young siliques (Le Jean et al., 2005). In rice, *OsYSL2* is expressed in the companion cells and phloem of leaves (Koike et al., 2004). Transcripts of *TcYSL3* and *TcYSL7* are localized in the central cylinder of young roots, the phloem of older roots, and, in the case of *TcYSL7*, in the phloem of the stem (Gendre et al., 2007). However, *OsYSL16* is also expressed in the mesophyll, suggesting its role for Fe-utilization in many cell types.

Arabidopsis IRT1 and rice *OsIRT1* and *OsYSL15* are expressed strongly in the outer tissues of the roots, including root hairs and epidermis, especially under Fe-deficiency, thereby playing a role in iron-uptake from the soil (Ishimaru et al., 2006; Lee et al., 2009; Vert et al., 2002). However, we did not see such expression by *OsYSL16* in the root epidermal cells. Furthermore, enhanced expression of that gene could not increase Fe levels in the vegetative tissues and mature seeds from that found under normal growing conditions. Therefore, all of our results allow us to postulate that the primary function of OsYSL16 for Fe-homeostasis is in distributing iron within a plant.

Note: Supplementary information is available on the Molecules and Cells website (www.molcells.org).

ACKNOWLEDGMENTS

We thank Kyungsook An and In-Soon Park for generating the transgenic lines, and Priscilla Licht for English editing of the manuscript. This work was supported in part by grants from the Next-Generation BioGreen 21 Program (No. PJ008215), Rural Development Administration, Republic of Korea; the Basic Research Promotion Fund, Republic of Korea (KRF-2007-341-C00028); Kyung Hee University (20110269); and the U.S. National Science Foundation Plant Genome Program (DBI-0701119 to M.L.G.).

REFERENCES

An, G., Ebert, P.R., Mitra, A., and Ha, S.B. (1988). Binary vectors. In Plant Molecular Biology Manual, S.B. Gelvin, and R.A. Schilperoort, eds. (Dordrecht, Kluwer Academic Publishers), pp. *A3*, 1-19.

An, S., Park, S., Jeong, D.H., Lee, D.Y., Kang, H.G., Yu, J.H., Hur, J., Kim, S.R., Kim, Y.H., Lee, M., et al. (2003). Generation and analysis of end sequence database for T-DNA tagging lines in rice. Plant Physiol. *133*, 2040-2047.

Aoyama, T., Kobayashi, T., Takahashi, M., Nagasaka, S., Usuda, K., Kakei, Y., Ishimaru, Y., Nakanishi, H,, Mori, S., and Nishizawa, N.K. (2009). OsYSL18 is a rice Fe(III)-deoxymugineic acid transporter specifically expressed in reproductive organs and phloem of lamina joints. Plant Mol. Biol. *70*, 681-692.

Arnon, D.I. (1949). Copper enzymes in isolated chloroplasts: Polyphenoloxidase in *Beta vulgaris*. Plant Physiol. *24*, 1-15.

Basso, B., Bagnaresi, P., Bracale, M., and Soave, C. (1994). The yellow-stripe-1 and -3 mutants of maize: nutritional and biochemical studies. Maydica *39*, 97-105.

Chu, H.H., Chiecko, J., Punshon, T., Lanzirotti, A., Lahner, B., Salt, D.E., and Walker, E.L. (2010). Successful reproduction requires the function of Arabidopsis Yellow Stripe-Like1 and Yellow Stripe-Like3 metal-nicotianamine transporters in both vegetative and reproductive structures. Plant Physiol. *154*, 197-210.

Colangelo, E.P., and Guerinot, M.L. (2006). Put the metal to the petal, metal uptake and transport throughout plants. Curr. Opin. Plant Biol. *9*, 322-330.

Curie, C., Panaviene, Z., Loulergue, C., Dellaporta, S.L., Briat, J.F., and Walker, E.L. (2001). Maize *yellow stripe*1 encodes a membrane protein directly involved in Fe (III) uptake. Nature *409*, 346-349.

Di Donato, R.J., Roberts, L.A., Sanderson, T., Eisley, R.B., and Walker, E.L. (2004). *Arabidopsis* Yellow Stripe-like2 (YSL2): a metal-regulated gene encoding a plasma membrane transporter of nicotianamine-metal complexes. Plant J. *39*, 403-414.

Gendre, D., Czernic, P., Conejero, G., Pianelli, K., Briat, J.F., Lebrun, M., and Mari, S. (2007). *TcYSL3*, a member of the YSL gene family from the hyper-accumulator *Thlaspi caerulescens*, encodes a nicotianamine-Ni/Fe transporter. Plant J. *49*, 1-15.

Goff, S.A., Ricke, D., Lan, T.H., Presting, G., Wang, R., Dunn, M., Glazebrook, J., Sessions, A., Oeller, P., Varma, H., et al. (2002). A draft sequence of the rice genome (*Oryza sativa* L. ssp. *japonica*). Science *296*, 92-100.

Guerinot, M.L., and Yi, Y. (1994). Iron: nutritious, noxious and not readily available. Plant Physiol. *104*, 815-820.

Harrison, P.M., and Arosio, P. (1996). The ferritins: molecular properties, iron storage function and cellular regulation. Biochim. Biophys. Acta *1275*, 161-203.

Henriques, R., Jasik, J., Klein, M., Martinoia, E., Feller, U., Schell, J., Pais, M.S., and Koncz, C. (2002). Knock-out of *Arabidopsis* metal transporter gene IRT1 results in iron deficiency accompanied by cell differentiation defects. Plant Mol. Biol. *50*, 587-597.

Inoue, H., Kobayashi, T., Nozoye, T., Takahashi, M., Kakei, Y., Suzuki, K., Nakazono, M., Nakanishi, H., Mori, S., and Nishizawa, N.K. (2009). Rice OsYSL15 is an iron-regulated iron(III)-deoxymugineic acid transporter expressed in the roots and is essential for iron uptake in early growth of the seedlings. J. Biol. Chem. *284*, 3470-3479.

Ishimaru, Y., Suzuki, M., Tsukamoto, T., Suzuki, K., Nakazono, M., Kobayashi, T., Wada, Y., Watanabe, S., Matsuhashi, S., Takahashi, M., et al. (2006). Rice plants take up iron as an Fe^{3+}-phytosiderophore and as Fe^{2+}. Plant J. *45*, 335-346.

Ishimaru, Y., Masuda, H., Bashir, K., Inoue, H., Tsukamoto, T., Takahashi, M., Nakanishi, H., Aoki, N., Hirose, T., Ohsugi, R., et al. (2010). Rice metal-nicotianamine transporter, OsYSL2, is required for the long-distance transport of iron and manganese. Plant J. *62*, 379-390.

Jeong, D.H., An, S., Park, S., Kang, H.G., Park, G.G., Kim, S.R., Sim, J., Kim, Y.O., Kim, M.K., Kim, S.R., et al. (2006). Generation of a flanking sequence-tag database for activation-tagging lines in japonica rice. Plant J. *45*, 123-132.

Kang, H.G., Jeon, J.S., Lee, S., and An, G. (1998). Identification of class B and class C floral organ identity genes from rice plants. Plant Mol. Biol. *38*, 1021-1029.

Koike, S., Inoue, H., Mizuno, D., Takahashi, M., Nakanishi, H., Mori, S., and Nishizawa, N.K. (2004). OsYSL2 is a rice metal-nicotianamine transporter that is regulated by iron and expressed in the phloem. Plant J. *39*, 415-424.

Lee, S., and An, G. (2009). Overexpression of *OsIRT1* leads to increased iron and zinc accumulations in rice. Plant Cell Environ. *32*, 408-416.

Lee, S., Jeon, J.S., Jung, K.H., and An, G. (1999) Binary vector for efficient transformation of rice. J. Plant Biol. *42,* 310-316.

Lee, S., Chiecko, J.C., Kim, S.A., Walker, E.L., Lee, Y., Guerinot, M.L., and An, G. (2009). Disruption of OsYSL15 leads to iron inefficiency in rice plants. Plant Physiol. *150*, 786-800.

Le Jean, M., Schikora, A., Mari, S., Briat, J.F., and Curie, C. (2005). A loss-of-function mutation in AtYSL1 reveals its role in iron and nicotianamine seed loading. Plant J. *44*, 769-782.

Marschner, H., and Römheld, V. (1994). Strategies of plants for acquisition of iron. Plant Soil. *165*, 375-388.

Mori, S. (1999). Iron acquisition by plants. Curr. Opin. Plant Biol. *2,* 250-253.

Murata, Y., Ma, J.F., Yamaji, N., Ueno, D., Nomoto, K., and Iwashita, T. (2006). A specific transporter for iron(III)-phytosiderophore in barley roots. Plant J. *46*, 563-572.

Roberts, L.A., Pierson, A.J., Panaviene, Z., and Walker, E.L. (2004). Yellow stripe1: expanded roles for the maize iron-phytosiderophore transporter. Plant Physiol. *135*, 112-120.

Robinson, N.J., Procter, C.M., Connolly, E.L., and Guerinot, M.L. (1999). A ferric-chelate reductase for iron uptake from soils. Nature *397*, 694-697.

Römheld, V., and Marschner, H. (1986). Evidence for a specific uptake system for iron phytosiderophores in roots of grasses. Plant Physiol. *80*, 175-180.

Schaaf, G., Ludewig, U., Erenoglu, B.E., Mori, S., Kitahara, T., and von Wirén, N. (2004). ZmYS1 functions as a proton-coupled symporter for phytosiderophore- and nicotianamine-chelated

metals. J. Biol. Chem. *279*, 9091-9096.
Schaaf, G., Schikora, A., Haberle, J., Vert, G., Ludewig, U., Briat, J.F., Curie, C., and von Wirén, N. (2005). A putative function for the *Arabidopsis* Fe-phytosiderophore transporter homolog AtYSL2 in Fe and Zn homeostasis. Plant Cell Physiol. *46*, 762-774.
Varotto, C., Maiwald, D., Pesaresi, P., Jahns, P., Salamini, F., and Leister, D. (2002). The metal ion transporter IRT1 is necessary for iron homeostasis and efficient photosynthesis in *Arabidopsis thaliana*. Plant J. *31*, 589-599.
Vert, G., Grotz, N., Dedaldechamp, F., Gaymard, F., Guerinot, M.L., Briat, J.F., and Curie, C. (2002). IRT1, an *Arabidopsis* transporter essential for iron uptake from the soil and for plant growth. Plant Cell. *14*, 1223-1233.
Vert, G., Barberon, M., Zelazny, E., Séguéla, M., Briat, J.F., and Curie, C. (2009). *Arabidopsis* IRT2 cooperates with the high-affinity iron uptake system to maintain iron homeostasis in root epidermal cells. Planta *229*, 1171-1179.
Waters, B.M., Chu, H.H., Di Donato, R.J., Roberts, L.A., Eisley, R.B., Lahner, B., Salt, D.E., and Walker, E.L. (2006). Mutations in *Arabidopsis yellow stripe-like1* and *yellow stripe-like3* reveal their roles in metal ion homeostasis and loading of metal ions in seeds. Plant Physiol. *141*, 1446-1458.
Yu, J., Hu, S., Wang, J., Wong, G.K., Li, S., Liu, B., Deng, Y., Dai, L., Zhou, Y., Zhang, X., et al. (2002). A draft sequence of the rice genome (*Oryza sativa* L. ssp. *indica*). Science *296*, 79-92.